Available online at www.sciencedirect.com

ScienceDirect

IFAC PapersOnLine 59-5 (2025) 13–18

Gear shift optimization for minimizing CO_2 emissions of a diesel-hydrogen fueled truck

Mats Versmissen * **Frank Willems** *,** **Daniel Pearce** ***

* *Control Systems Technology, Eindhoven University of Technology, Netherlands (e-mail: m.versmissen@tue.nl)*
** *TNO Mobility and Built Environment, Netherlands*
*** *CMB.TECH, United Kingdom*

Abstract: This research aims to minimize CO_2 emissions of a retro-fitted diesel-hydrogen fueled truck by optimizing the gear shift strategy of its standard sixteen-speed automated manual transmission. The approach involves developing a dynamic programming algorithm aimed at maximizing diesel displacement by hydrogen for a given drive cycle, while taking driveability metrics into account. The developed gear shift strategy controls the gear position and shifts the engine operating region towards a high torque-low engine speed region, more favorable for hydrogen injection. The gear shift optimization is performed for the mono-fuel diesel engine map, serving as a baseline, and for the dual-fuel engine map. The theoretical reduction in CO_2 emissions ranged from 1.3% up to 4.6%, depending on the vehicle payload and the drive cycle under consideration. Furthermore, the algorithm is used to generate real-time implementable shift maps designed to maximize dual-fuel efficiency for unknown drive cycles. Implementing the dual-fuel shift maps led to a reduction in CO_2 emissions, spanning from 0.8% to 2.6%, in comparison to the mono-fuel optimized shift map. This reduction of 2.6% was observed near the maximum allowable payload of 20 tonnes.

Keywords: Dual-fuel engines, drivetrain modeling, optimal control, dynamic programming

1. INTRODUCTION

The transportation sector is a significant contributor to greenhouse gas emissions. Although heavy-duty vehicles represent less than 8% of the total number of vehicles on the road, they account for up to 35% of CO_2 emissions, and this figure continues to rise International Energy Agency (2023). For heavy-duty applications such as trucks, marine vessels, and construction equipment, transitioning to electrified powertrains in the near future appears overly optimistic, as it will require a significant expansion of infrastructure and further advancements in battery technology to compete with the well-matured internal combustion engine (ICE). Therefore, developing clean and efficient powertrain control strategies is crucial to meet future emission reduction targets. In addition to changing the powertrain layout, which has already demonstrated substantial reductions in CO_2 emissions, as shown in Moghadasi et al. (2024), the adoption of advanced combustion strategies can further facilitate these reductions. One promising concept is the co-combustion of hydrogen and diesel, which effectively lowers all carbonaceous emissions compared to conventional diesel engines Hosseini et al. (2023). The current generation of heavy-duty trucks can be retrofitted with a hydrogen injection system to support this dual-fuel combustion concept without losing the ability to run on diesel only Shahpouri et al. (2023). Achieving the best balance between efficiency and emissions in dual-fuel mode requires modifications to the air and fuel path controls Saravanan et al. (2007); Talibi et al. (2017). In addition to modifying the engine controls, re-calibration of the gear shift strategy can further enhance dual-fuel efficiency. Ngo et al. (2013) optimizes the gear position of a conventional vehicle over a specified drive profile, considering both fuel consumption and driveability. Ngo et al. (2014) extends this method, resulting in a sub-optimal feedforward gear shift map, by using a data-based approach. Both methods apply a dynamic programming (DP) algorithm to generate the optimal gear shift points.

This paper presents a dynamic programming approach that minimizes engine-out CO_2 emissions while taking driveability into account during optimization. The calculation of the optimal gear position is non-recursive and therefore, significantly requires less computational effort. The developed gear shift strategy is later applied to create a real-time (RT) implementable shift map which can be used to enhance dual-fuel engine operation.

The structure of this paper is as follows: first, a system description of all the related vehicle components is provided. Next, the DP optimization algorithm is presented alongside the method used for generating ideal shift lines. Following, simulation results are compared for both known and unknown drive cycles. Finally, the conclusion summarizes the findings.

2. SYSTEM DESCRIPTION

The studied heavy-duty truck features a 12.7-liter turbocharged Ecotorq engine running in either mono-fuel (diesel only) or dual-fuel (diesel - hydrogen) mode and is equipped with automated manual transmission (AMT).

Peer review under responsibility of International Federation of Automatic Control.
10.1016/j.ifacol.2025.07.074

This gearbox consists of 16 distinct gear positions with fixed gear ratios. Figure 1 illustrates the powertrain layout.

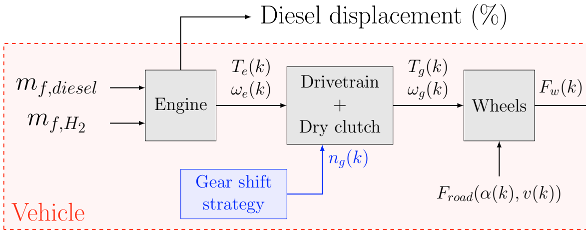

Fig. 1. Powertrain layout of the studied heavy-duty dual-fuel truck.

2.1 Engine

Engine fuel consumption is modeled as a static fuel map, which is calibrated based on stationary experiments conducted on an engine dynamometer. The hydrogen injection map is calibrated by injecting the maximum amount of hydrogen without exceeding certain combustion constraints, such as maximum pressure, peak pressure rise rate, and detonation limits. The standard engine ECU compensates for the additional torque generated by the diesel-hydrogen combustion by reducing the amount of diesel fuel injected at this set point. The static fuel maps for the dual-fuel engine are shown in Figure 2 as a static pointwise function of engine speed (ω_e) and engine torque (T_e). The engine speed is constrained within a specified range, and the torque is limited by a nonlinear torque constraint. These constraints are expressed as follows:

$$\omega_{e,min} \leq \omega_e(k) \leq \omega_{e,max} \tag{1}$$
$$0 \leq T_e(k) \leq T_{e,max}(\omega_e(k)) \tag{2}$$

where $\omega_{e,min}$ and $\omega_{e,max}$ are the minimum and maximum engine speeds, respectively. k denotes the discrete timestep of the algorithm and $T_{e,max}(\omega_e(k))$ the maximum engine output torque as a function of the current engine speed. During periods of deceleration, no fuel is consumed; therefore, engine braking is omitted from this study.

In addition, a new term, diesel displacement (DD), is introduced for the engine operating in dual-fuel mode. Diesel displacement is defined as the reduction of diesel fuel consumption between the engine running in dual-fuel mode and mono-fuel mode. The diesel displacement is calculated according to:

$$\mathrm{DD}(T_e(k), \omega_e(k)) = 1 - \frac{\dot{m}_{f,diesel,DF}}{\dot{m}_{f,diesel,MF}} \tag{3}$$

where $\dot{m}_{f,diesel,DF}$ represents the diesel fuel mass flow rate in dual-fuel mode and $\dot{m}_{f,diesel,MF}$ $[kg/h]$ represents the diesel fuel mass flow rate in mono-fuel mode. The diesel displacement metric is a measure for the CO_2 reduction potential when operating in dual-fuel engine mode.

2.2 Drivetrain

The mechanical power conversions within the gearbox are determined by the mathematical relationships presented below. These equations are functions of engine speed and the current gear ratio (i_g), which is dependent on the

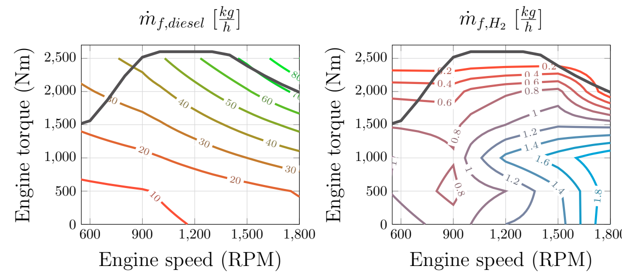

Fig. 2. Static fuel maps (contour) for the engine running in dual-fuel mode (Left: diesel fuel mass rate ($\dot{m}_{f,diesel,DF}$), right: hydrogen fuel mass rate ($\dot{m}_{f,hydrogen,DF}$)) with a maximum engine torque constraint (black). The absolute minimum engine speed is set at 550 RPM and the maximum engine speed is given as 1800 RPM.

selected gear position ($n_g(k)$) determined by the optimization algorithm.

$$\omega_e(k) = \omega_g(k) i_g(n_g(k)) \tag{4}$$

An efficiency term is incorporated into the torque conversion step, accounting for the mechanical losses that occur within the gearbox and the friction losses within the dry clutch ($\eta_{total} = \eta_{gearbox} \cdot \eta_{clutch}$), which connects the gearbox to the engine.

$$T_e(k) = \frac{T_g(k)}{\eta_{total} i_g(n_g(k))} \tag{5}$$

The gearbox behavior is governed through the difference equations $n_g(k+1) = n_g(k) + u(k)$ where $u(k)$ is the shift command, $n_g(k)$ is the current gear position and $n_g(k+1)$ equals the gear position at the next time step with gear position constraints:

$$1 \leq n_g(k) \leq 16 \tag{6}$$

and n_g can only take discrete values. The propulsion force driving the vehicle forward is given by:

$$F_w(k) = \frac{T_g(k)}{r_w} = \eta_{total} i_g(n_g(k)) \frac{T_e(k)}{r_w} \tag{7}$$

with r_w the tire radius.

2.3 Vehicle dynamics

The vehicle acceleration follows from Newton's second law of motion:

$$dv(k) = \frac{1}{m}(F_w(k) - F_{road}(k))\Delta t \tag{8}$$

with total vehicle mass m. The road load is given by:

$$\begin{aligned} F_{road}(k) &= \frac{1}{2} C_d A_f v(k)^2 \\ &\quad + mg[C_r cos(\alpha(k)) + sin(\alpha(k))] \end{aligned} \tag{9}$$

with α the road inclination of the drive cycle. The main vehicle parameters are defined in Table 1.

3. GEAR SHIFT OPTIMIZATION

3.1 Optimization problem

This work aims to optimize the gear shift strategy for a given dual-fuel vehicle, such that CO_2 emissions are minimized by reducing diesel fuel consumption (FC).

Table 1. Main vehicle parameters

Vehicle component	Parameter
Fuel type	diesel or diesel - hydrogen
Transmission	16-speed AMT, dry clutch
Gear ratios i_g	$[17.03, 14.1, 11.99, 9.93, 7.97, 6.6, 5.46, 4.52, 3.76, 3.12, 2.65, 2.19, 1.716, 1.46, 1.2, 1]$
Empty vehicle mass m	15779 [kg]
Maximum payload	20000 [kg]
Tire radius r_w	0.2 [m]
Frontal area A_f	9.974 [m^2]
Air drag coefficient C_d	0.6 [-]
Rolling resistance coefficient C_r	0.008 [-]
Drivetrain efficiency η_{total}	95 [%]

Given a speed and acceleration profile of a drive cycle, find the optimal gear shifting pattern $u^*(k) = u_g(k)$ for the discrete system $n_g(k+1) = n_g(k) + u_g(k)$ that minimizes FC according to:

$$u^*(k) = \underset{u_g(k)\in\mathcal{U}_g}{\text{argmin}}\ J_{k\to k+1} \tag{10a}$$

$$\text{s.t.} \quad 1 \leq n_g(k) \leq 16 \tag{10b}$$

with $J_{k\to k+1}$ the step cost, denoted as

$$J_{k\to k+1} = FC[\tilde{n}_g(k+1), k+1] + C(\tilde{n}_g(k+1)) \tag{11}$$

where $FC[\tilde{n}_g(k+1), k+1]$ presents the fuel consumption of the possible future state $\tilde{n}_g(k+1)$ and $C(\tilde{n}_g(k+1))$ a penalty imposed onto a gear shift action. The gear position or system state $n_g(k)$ is bounded and $u_g(k) \in \mathcal{U}_g$ presents the set of admissible inputs at time k for $\mathcal{U}_g = \{-2, -1, 0, 1, 2\}$. The optimization problem is solved using a dynamic programming approach, presented in the following subsection.

3.2 Dynamic programming

The approach of calculating the optimal gear shift pattern for a specific drive cycle can be written as:

(1) Discretize the reference velocity and acceleration profile.
(2) Create a mesh grid $FC \in \mathbb{R}^{n_g \times N}$, with N the length of the drive cycle, and assign the associated system state $n_g(k)$ to each individual coordinate within the mesh grid.
(3) For every grid point, perform a backwards calculation:
  (a) Determine the required engine speed $\omega_e(k)$ to attain the velocity reference $v(k)$ at every possible gear position $n_g(k)$.
  (b) Determine the required engine torque $T_e(k)$ to reach the consecutive state for every possible gear position.
  (c) Set the grid points that do not abide by the engine constraints ($T_{e,max}, \omega_{e,min/max}$) as unreachable: $FC[n_g, k] = \text{Inf}$.
  (d) Assign a fuel rate ($\dot{m}_{f,diesel}$) to each grid point using $\omega_e(k)$ and $T_e(k)$.
(4) Step across the complete mesh grid and determine the consecutive system state $n_g(k+1)$ based on the lowest step cost:

$$\begin{aligned} J_{k\to k+1} = FC[\tilde{n}_g(k+1), k+1] \\ + C(\tilde{n}_g(k+1)) \end{aligned} \tag{12}$$

where the possible future states $\tilde{n}_g(k+1)$ are:

$$\tilde{n}_g(k+1) = n_g(k) + \mathcal{U}_g \tag{13a}$$

$$\text{s.t.} \quad 1 \leq \tilde{n}_g(k) \leq 16 \tag{13b}$$

The step cost $J_{k\to k+1}$ consists of two separate parts. First, the fuel cost of the potential future states $FC\big[\tilde{n}_g(k+1), k+1\big]$, stored inside the mesh grid. Second, $C(\tilde{n}_g(k+1))$ is a penalty imposed on gear shift actions, given as

$$C(\tilde{n}_g(k+1)) = \begin{cases} 0, & \text{if } \tilde{n}_g(k+1) = n_g(k) \\ \beta \cdot FC(\tilde{n}_g(k+1), k+1), & \text{if } \tilde{n}_g(k+1) \neq n_g(k) \end{cases} \tag{14}$$

representing a fraction ($\beta = 0.01$) of the fuel cost of adjacent gear positions, placing a penalty on switching gears. The addition of $C(\tilde{n}_g(k+1))$ ensures that the benefit of switching gears results in a substantial improvement of the engine's fuel efficiency.

The presented dynamic programming approach differs from other algorithms in that it only needs to find the optimal solution for a single future state and not over a finite time horizon, thereby reducing computational complexity van Schijndel et al. (2014). The shift penalty $C(\tilde{n}_g(k+1))$ ensures that the number of shifts is reduced during optimization over the complete drive cycle, which can be controlled by tuning the β-value.

The reference drive cycle is discretized with a sampling frequency of 1 Hz, corresponding to a time step of 1 second. This sampling rate allows the dynamics associated with gear position changes, such as shift delays, to be disregarded.

3.3 Real-time implementable shift map

The proposed optimization algorithm in subsection 3.2 is designed to create a shift pattern over a known drive cycle, aiming to minimize the accumulated diesel fuel consumption. Additionally, this algorithm can be used to generate real-time implementable feedforward shift maps, which will result in a sub-optimal shift pattern for an unknown drive cycle. These shift maps aim to approximate the gear shift strategy from the DP algorithm for unknown drive cycles.

Approach:

(1) Acquire shift data from different drive cycle simulations and various payloads. Categorize each individual upshift and downshift event.
(2) Visually inspect the data and remove potential outliers to create a generalized shift cloud.
(3) Use a combination of hierarchical and k-means clustering methods to generate centroids that form the backbone of the shift line. Ikotun et al. (2023)
(4) Connect the centroids and extrapolate them towards the engine's torque limit constraint.

This approach is visualized in Figure 3 for the optimized upshift event from $n_g : 15 \to 16$ for the engine in running mono-fuel mode. Every dot represents an upshift action for

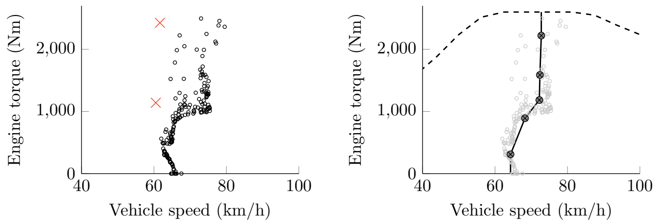

Fig. 3. Extracting a single shift line from optimal gear shift actions. Left: obtaining shift data from multiple drive cycles and removing outliers (×). Right: Constructing optimal shift line by connecting centroids (⊗) and extrapolate towards the torque limit (dashed).

an arbitrary drive cycle calculated using DP. These maps approximate the fuel economy savings and the driveability metrics from the dynamic programming algorithm.

4. SIMULATION RESULTS

This section presents the simulation results for various drive cycles (Table 2) and applies these results to generate the sub-optimal feedforward shift maps as described in subsection 3.3. The improvements in diesel displacement are based on a comparison between two dual-fuel vehicles: the first vehicle implements the strategy 'as is', which is optimized for a mono-fuel engine, while the second vehicle uses an optimal shift strategy for the dual-fuel engine map. Initially, the arterial segment of the Transit Coach Operating Duty Cycle (Figure 4) is used to validate the plain dynamic programming algorithm. Subsequently, the shift maps are introduced, and the results of additional cycles, optimized with the DP algorithm (DP optimized) are presented alongside those which are optimized using the shift maps (Real-time optimized).

For these simulations, the lower engine speed limit is set at 600 RPM to prevent the engine from running too close to idle (550 RPM) and increase drive comfort. Three individual load cases are simulated to cover a wider range of required engine power for the various drive cycles. The first case is a simulation with no additional payload, followed by a medium payload of 10 tons and a heavy payload of 20 tons. The vehicle with the additional 20-ton payload comes close to the maximum gross vehicle weight (40 tons) allowed on European roads for trucks up to 16.5 meters in length. Katsarova (2014)

4.1 Optimized gear shift strategy using DP

The optimized shift patterns for the arterial segment of the Transit Coach Operating Duty Cycle are shown in Figure 4 for a payload of 20 tons. This figure displays the optimal gear position sequences for both the mono-fuel and dual-fuel DP optimized shift strategies, illustrating the differences in shift decisions for a single drive cycle segment. The improvements in diesel displacement achieved by these different shift strategies range from a 5.8% improvement for the case with no additional payload, to improvements of 2.8% and 2.4% for the 10-ton and 20-ton payload, respectively. These improvements can be directly linked to the different engine operating areas as the operating point is controlled and manipulated through

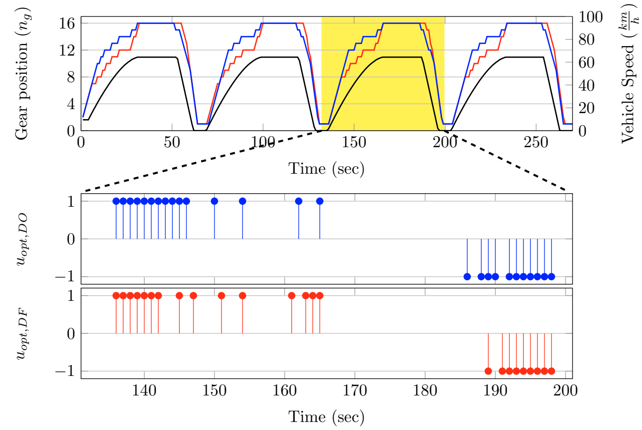

Fig. 4. DP optimized shift strategy for mono-fuel (blue) and dual-fuel (red) operation assuming a payload of 20 tons for uniform velocity profile (black): single drive cycle segment extracted to visualize differences in shift decisions.

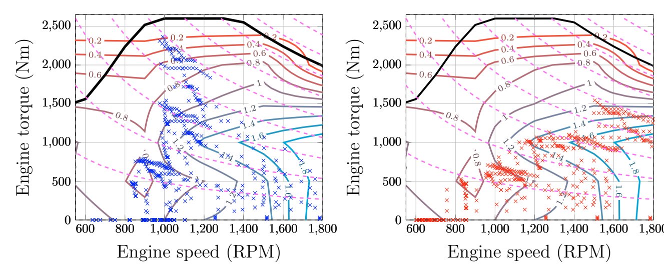

Fig. 5. The mono-fuel strategy (blue) aligns the engine operating region to maximize engine efficiency while the dual-fuel strategy (red) is optimized along maximum hydrogen injection at high engine output power (pink, dashed). Simulation performed for no payload, 10 and 20 tons.

gear selection. Figure 5 illustrates this, where the mono-fuel gear shift strategy fails to place the engine operating points near the most fuel-optimal region for hydrogen injection, the dual-fuel strategy successfully achieves this optimal alignment.

The results of these simulations indicate that the dynamic programming algorithm effectively maximizes hydrogen injection over a known drive profile. This optimization leads to higher diesel displacement values, resulting in a significantly lower overall CO_2 emission rate.

4.2 Development of real-time shift maps using optimized shift data obtained from DP

Optimal shift decisions, as shown in Figure 4, are used as input data to create real-time shift maps. By evaluating a sufficient number of drive cycles with varying load profiles, a large set of optimal shift decisions across the entire engine map is obtained, which is then used to derive the shift maps. A fixed number of 5 clusters for the k-means algorithm is considered to generate all the shift lines.

The additional drive cycles from Table 2 are simulated for the three payload cases, resulting in an accumulated driving time of 5 hours and 21 minutes to generate the shift maps shown in Figure 6.

Table 2. Drive cycles representative for various heavy-duty transport scenarios from National Renewable Energy Laboratory (NERL) (2023). (a)-(e) used for real-time map development.

	Drive cycle name	**Duration**	**Maximum Speed**	**Mean Speed**	**Mean Acceleration**	**Kinetic intensity**	**Number of stops**
		Minutes	km/h	km/h	m/s^2	1/km	
	Arterial Segment of the Transit Coach Operating Duty Cycle	4.5	64	41.6	0.405	0.802	4
a.	City Suburban Heavy Vehicle Cycle (CSHVC)	28.33	70.08	22.88	0.314	1.119	13
b.	CARB Heavy Heavy-Duty Diesel Truck (HHDDT) Cruise Segment	34.73	94.88	63.77	0.082	0.075	6
c.	CARB Heavy Heavy-Duty Diesel Truck (HHDDT) Transient Segment	11.13	76.01	24.57	0.298	0.863	4
d.	Urban Dynamometer Driving Schedule for Heavy-Duty Vehicles (UDDS HD)	17.68	92.81	30.14	0.274	0.381	14
e.	NREL Refuse Truck Cycle (Miama-Dade)	15.02	84.43	12.38	0.423	0.818	20

Both strategies implement a fixed RPM upshift and downshift control action because the drive cycle data was not extensive enough to accurately predict the optimal shift line for these gear positions. The fixed RPM strategy is implemented from gear $n_g : 1 \rightarrow 7$ for the mono-fuel map and $n_g : 1 \rightarrow 5$ for the dual-fuel map. This method has been applied for both up- and downshift lines. Since the double up- and downshift control actions ($u_g = \{-2, 2\}$) were rarely seen as optimal, these data points were omitted from the analysis as well. The shape of both shift maps

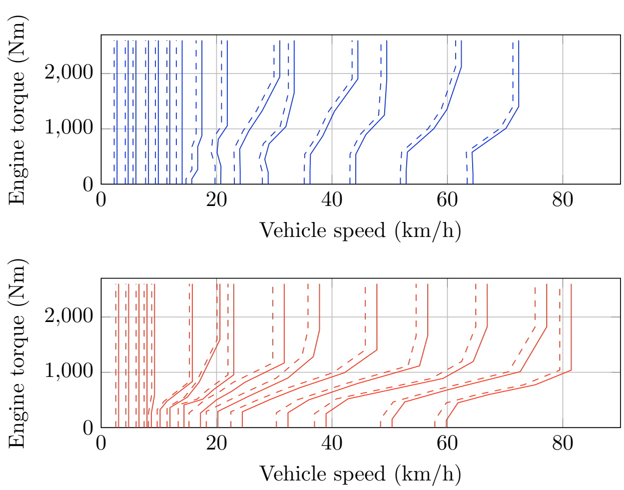

Fig. 6. Sub-optimal shift maps for mono-fuel (blue) operation and dual-fuel (red) operation. The fixed RPM decision is indicated as a straight vertical line. The dashed lines represent the downshift action.

varies significantly for similar shift actions. The analysis of these differences is divided into two categories: high- and low engine load. At low engine load, a faster upshift is more desirable to keep the engine running at low engine speed, which is favorable for dual-fuel operation. In the higher load range, the shift actions are moved to higher vehicle speeds compared to the mono-fuel map. At higher loads, the upshift is delayed ensuring that the engine operates at high engine speed and low output torque, which is ideal for maximizing hydrogen injection and thus, maximizing diesel displacement. Besides the individual optimizations using DP, additional simulations are performed for each shift map. Although the real-time maps result in a less optimal approach, they remain more advantageous for dual-fuel operation when comparing the two shift maps side-by-side. We compare two dual-fuel vehicles, equipped with different shift strategies. The mono-fuel optimized control policy represents our baseline and we compare this with a dual-fuel optimized solution. This is done for the DP optimized and the the Real-time optimized shift policies. The results of simulating the drive cycles with a payload of 20 tons, which is the most critical for achieving improvements, are shown in Figure 7. The improvements in RT range from a minimum of 0.8% for the cruise segment to a maximum of 2.6% for the transient segment in the CARB heavy-duty cycle. This compares to 1.3 % and 4.6 % improvements for the DP optimization on the same drive cycles. The RT improvements are less significant, as they represent a sub-otpimal shift policy averaged over multiple drive cycles.

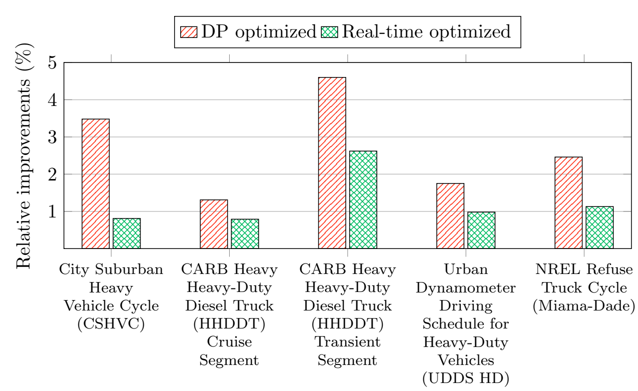

Fig. 7. Relative improvements in diesel displacement between mono-fuel shift strategy and dual-fuel optimized shift strategies (DP- and Real-time optimized). Vehicle payload equals 20 tons.

A high number of required accelerations leads to a larger amount of possible shift actions, facilitating increased hydrogen injection through an optimal shift decision. For drive cycles with a larger mean acceleration, the benefits of a modified gear shift strategy are emphasized more clearly. The optimal operating regions from the simulations are shown in Figure 8.

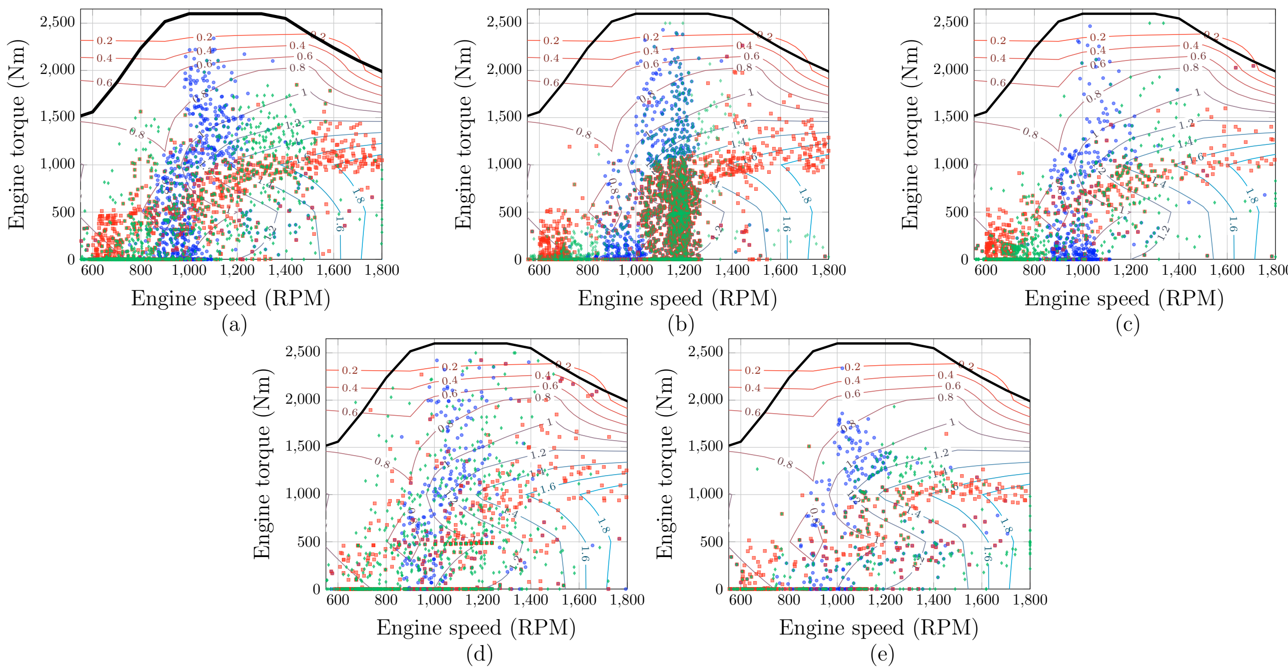

Fig. 8. Engine operating regions for simulated drive cycles are shown, highlighting optimized regions for a mono-fuel engine (blue, representing the baseline gear shift strategy of the truck) and a dual-fuel engine (red, optimized for retro-fitted truck). The engine operating region for the real-time dual-fuel shift map (green) approximates the ideal operating region for a dual-fuel engine. Vehicle payload equals 20 tons.

5. CONCLUSIONS

A dynamic programming algorithm has been developed to optimize the gear shift strategy and thereby, reducing CO_2 emissions of a dual-fuel heavy duty truck. This algorithm is used to generate real-time implementable shift maps that are able to decrease CO_2 emissions during vehicle operation. The relative increase between a mono-fuel and a dual-fuel optimized shift map were validated in a simulation environment. The simulation results varied between 0.8% and 2.6% for an assumed payload of 20 tons. The maximum increase in diesel displacement equal to 2.6% was achieved for the transient segment of the CARB heavy-duty cycle. The achievable improvements depend on each individual cycle and the required acceleration behavior of the vehicle. This study demonstrates the practical applicability of an optimized gear shift strategy by further decreasing CO_2 emissions of a dual-fuel vehicle in a real-world environment.

ACKNOWLEDGEMENTS

The authors thank CMB.TECH for providing the engine calibration and vehicle data used within this project.

REFERENCES

Hosseini, S.H., Tsolakis, A., Alagumalai, A., Mahian, O., Lam, S.S., Pan, J., Peng, W., Tabatabaei, M., and Aghbashlo, M. (2023). Use of hydrogen in dual-fuel diesel engines. *Progress in Energy and Combustion Science*, 98, 101100.

Ikotun, A.M., Ezugwu, A.E., Abualigah, L., Abuhaija, B., and Heming, J. (2023). K-means clustering algorithms: A comprehensive review, variants analysis, and advances in the era of big data. *Information Sciences*, 622, 178–210. doi:https://doi.org/10.1016/j.ins.2022.11.139.

International Energy Agency (2023). Net zero roadmap: A global pathway to keep the 1.5 °C goal in reach. Accessed: 25/02/2025.

Katsarova, I. (2014). Weights and dimensions of road vehicles in the eu. URL `https://www.europarl.europa.eu/RegData/bibliotheque/briefing/2014/140796/LDM_BRI(2014)140796_REV1_EN.pdf`. Accessed: 25/02/2025.

Moghadasi, S., Long, Y., Jiang, L., Munshi, S., McTaggart-Cowan, G., and Shahbakhti, M. (2024). Design and performance analysis of hybrid electric class 8 heavy-duty regional-haul trucks with a micro-pilot natural gas engine in real-world highway driving conditions. *Energy Conversion and Management*, 309, 118451.

National Renewable Energy Laboratory (NERL) (2023). Nrel drive-cat - chassis dynamometer drive cycles. URL `http://www.nrel.gov/transportation/drive-cycle-tool`. Accessed: 25/02/2025.

Ngo, V.D., Hofman, T., Steinbuch, M., and Serrarens, A. (2014). Gear shift map design methodology for automotive transmissions. *Proceedings of the Institution of Mechanical Engineers, Part D: Journal of Automobile Engineering*, 228(1), 50–72. doi:10.1177/0954407013506698.

Ngo, V.D., Navarrete, J.A.C., Hofman, T., Steinbuch, M., and Serrarens, A. (2013). Optimal gear shift strategies for fuel economy and driveability. *Proceedings of the Institution of Mechanical Engineers, Part D: Journal of Automobile Engineering*, 227(10), 1398–1413. doi:10.1177/0954407013491240.

Saravanan, N., Nagarajan, G., Dhanasekaran, C., and Kalaiselvan, K. (2007). Experimental investigation of hydrogen port fuel injection in di diesel engine. *International Journal of Hydrogen Energy*, 32(16), 4071–4080. TMS06: Symposium on Materials in Clean Power Systems.

Shahpouri, S., Gordon, D., Hayduk, C., Rezaei, R., Koch, C.R., and Shahbakhti, M. (2023). Hybrid emission and combustion modeling of hydrogen fueled engines. *International Journal of Hydrogen Energy*, 48(62), 24037–24053. doi:https://doi.org/10.1016/j.ijhydene.2023.03.153.

Talibi, M., Hellier, P., and Ladommatos, N. (2017). The effect of varying EGR and intake air boost on hydrogen-diesel co-combustion in CI engines. *International Journal of Hydrogen Energy*, 42(9), 6369–6383. doi:https://doi.org/10.1016/j.ijhydene.2016.11.207.

van Schijndel, J., Donkers, M., Willems, F., and Heemels, W. (2014). Dynamic programming for integrated emission management in diesel engines. *IFAC Proceedings Volumes*, 47(3), 11860–11865. doi:https://doi.org/10.3182/20140824-6-ZA-1003.02580. 19th IFAC World Congress.